Chapter 3

The Model

Contents

3.1 Choosing the RAMONA Model

Modeling BWR dynamics requires the simulation of the thermal-hydraulics and the neutronics as well as their mutual interactions. This involves the setting up and the solution of the partial differential equations describing the basic phenomenon. The interaction during instabilities in BWRs is shown in Figure 3.1.

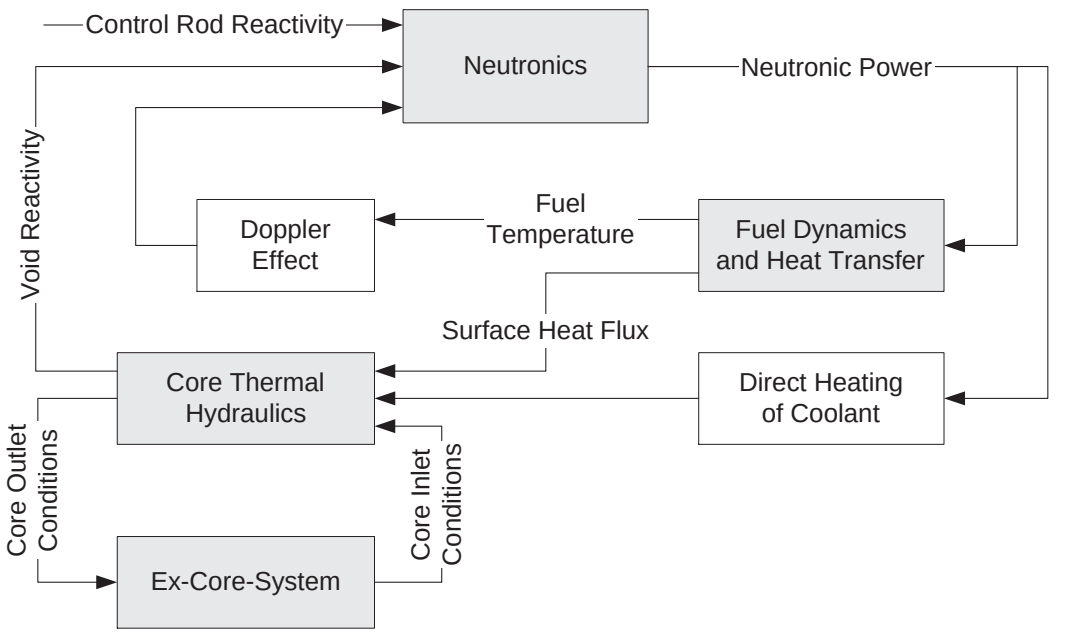

Figure 3.1: Neutronic/Thermal-Hydraulic Feedback System in a BWR

Four main interaction blocks can be noted:

- Core thermal hydraulics, which affects power production by fission and is often the trigger for instability mechanisms.
- Neutron kinetics, which is directly responsible for the power variation, as a consequence of the external and the feedback reactivity perturbations.
- Fuel dynamics and heat transfer, which act as a filter of power perturbations and introduce time delays between power production and coolant flow heating.
- Ex-core-systems which impose the boundary conditions to the core channels, thus influencing their stability.

As mentioned before, the physical model of MATSTAB was taken from RAMONA-3B. Naturally, MATSTAB does not contain all the features and details implemented in RAMONA

since the scope of transients to be analyzed is condensed from a wide variety to one only. Especially changes that happen in time, like the opening or closing of valves or the movement of control rods, are not meant to be modeled in MATSTAB.

To start with, it was not yet perfectly clear how good the new approach, was and to what detail one would be forced to go when using linear equations. Therefore, the RAMONA model was transferred in a one to one scope.

This means that not only the proven and established principles were mined out, but also some past sins as well as unnecessary burdens found their way into MATSTAB (e.g. a too detailed model for the fuel temperatures and some thermal hydraulic properties or different numbering schemes in the neutronic and thermal hydraulic part of the core).

Since MATSTAB was just a 1-D model at its very beginning, this overkill had no significant influence on the computational effort needed. Actually, the ability to compare the results of the two codes in a very direct manner was an intended and welcome benefit.

After everything went smooth in 1-D, MATSTAB was extended to handle 3-D neutronics and one thermal hydraulic channel per fuel assembly. The resulting explosion in demand for CPU power, and most important, system memory, made it necessary to simplify some of the equations. It goes without saying, that the simplifications were judged against their physical impact.

The following section presents some comments on the BWR reactor types implemented and an overview over the nodalization scheme, in order to give an impression of the scale and detail of the model. The subsequent sections address the major changes introduced by MATSTAB to the RAMONA-3B model. The complete model implemented in MATSTAB can be found in Appendix A.

For the sake of convenience, Appendix A is written like a normal chapter in its own right with detailed derivations. It can therefore be read as a whole, without flipping back and forth between Appendix A and Chapter 3. Consequently, all changes discussed below will also be found in Appendix A.

3.1.1 Nodalization Scheme

As mentioned before, MATSTAB was and still is developed at the Forsmark site in Sweden. The three Forsmark reactors were supplied by ABB. The Leibstadt NPP situated in Switzerland, which was integrated in the project later on, is a BWR6 supplied by GE. As far as modeling is concerned, the plants differ mainly in their pump types; internal pumps are used in Forsmark and jet pumps in Leibstadt (Figure 3.2).

Both pump types are part of the MATSTAB/RAMONA model. The other differences are mainly in their geometrical data which are supplied by the user in the file `parameter.inp`. Besides these differences in construction, the specification of the fuel, such as heat transfer coefficients and pressure drops over spacers, are also supplied as an input by the user.

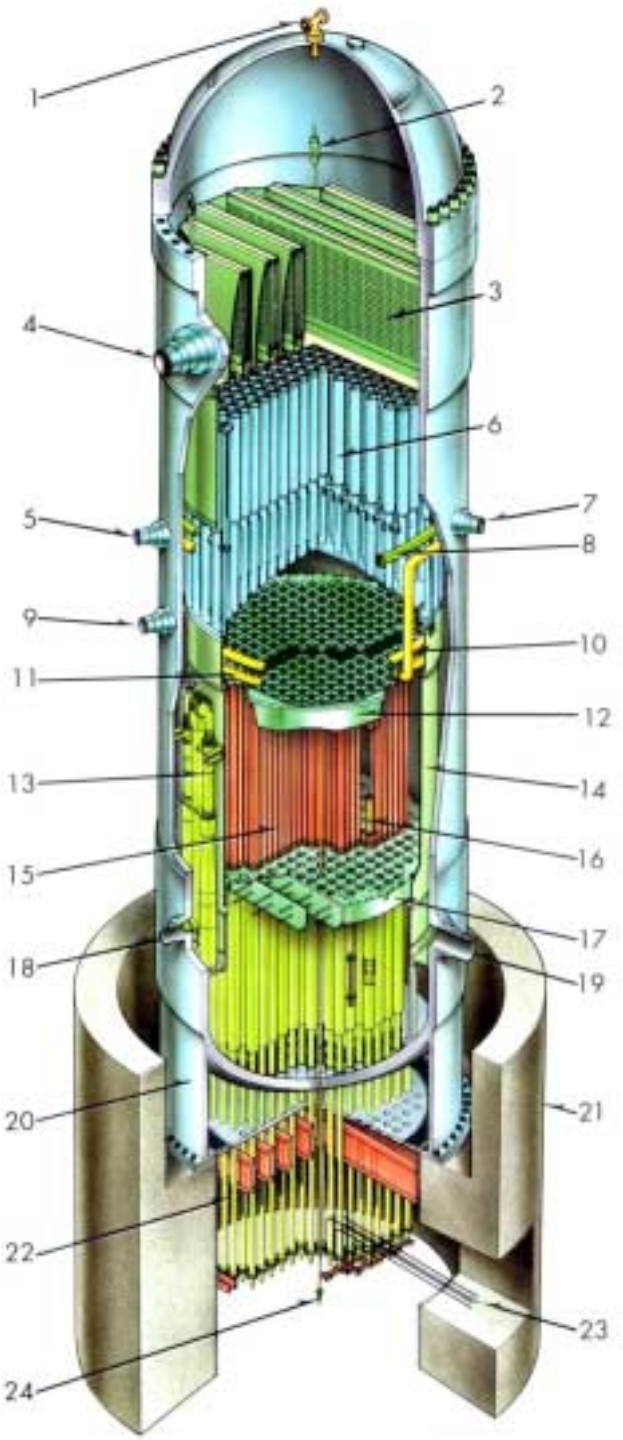

1. Vent and head spray
2. Steam dryer lifting lug
3. Steam dryer assembly
4. Steam outlet
5. Core spray inlet
6. Steam separator assembly
7. Feedwater inlet
8. Feedwater sparger
9. Low-pressure coolant injection inlet
10. Core spray line
11. Core spray sparger
12. Top guide
13. Jet pump assembly
14. Core shroud
15. Fuel assemblies
16. Control blade
17. Core plate
18. Recirculation water inlet
19. Recirculation water outlet
20. Vessel support skirt
21. Shield wall
22. Control rod drives
23. Control rod drive hydraulic lines
24. In-core flux monitor

Figure 3.2: The Leibstadt BWR6 Reactor

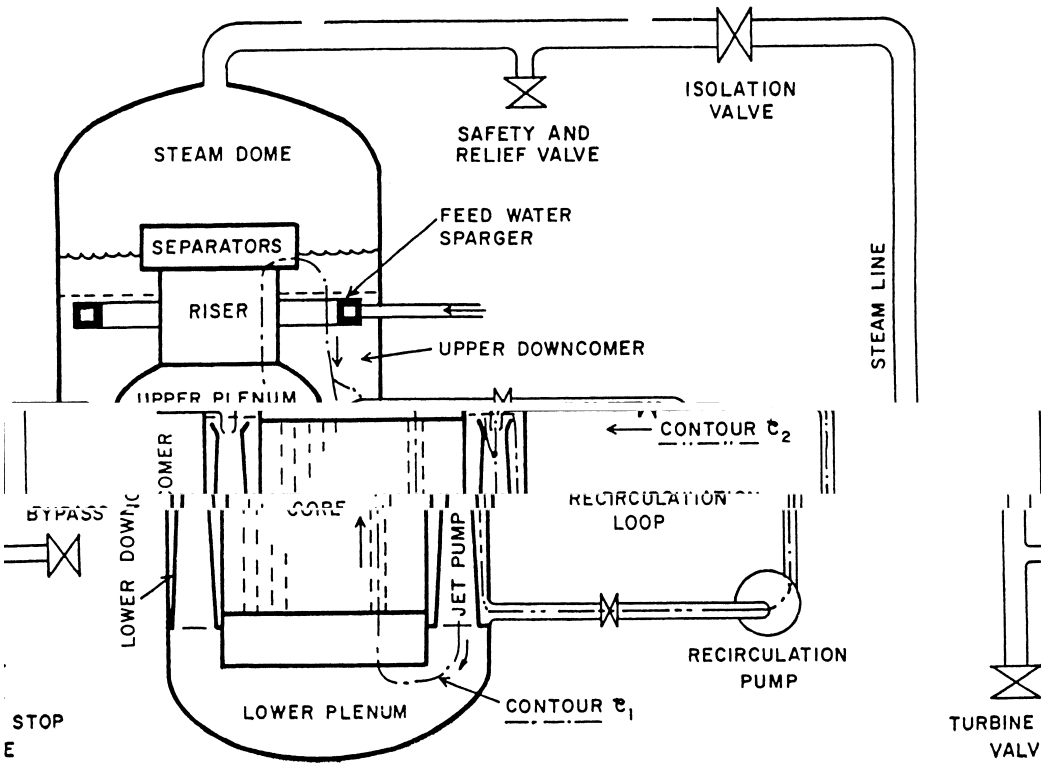

Figure 3.3: Schematic View of the Leibstadt Reactor

This allows MATSTAB to model a wide range of different boiling water reactors. A more schematic view of the reactor is shown in Figure 3.3.

The complete model is divided into 8 regions (downcomer 1&2, lower plena 1&2, core, bypass, riser, steam dome), each of which has an individual and variable number of nodes. In addition to these physical nodes, most sections also have a non physical entry-node containing the boundary conditions. The number of nodes in each section, as well as several parameters for each node, may be chosen by the user, see Figure 3.4.

The nodes are numbered counter-clockwise, beginning in the downcomer 1 and ending in the steam dome. Each core plane is subdivided into channels that coincide with the fuel assemblies. Within a plane, the numbering begins with channel 1 and ends with the bypass. The values in Figure 3.4 may be changed by the user. However, they should reflect the physical reality and remain the same for all cases. Only a major plant upgrade would introduce a change.

The only numbers which have to be adjusted annually are the parameters for the fuel, i.e. at the beginning of a cycle, when a new fuel type is introduced, its parameters have to be added to the parameter file.

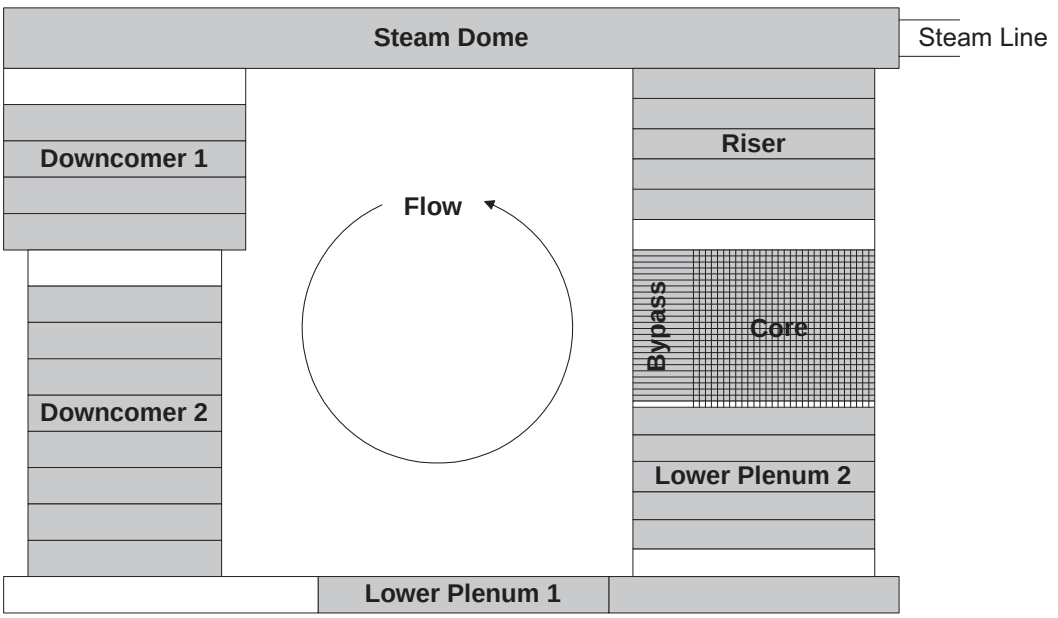

	Axial Nodes	Flow Area $[m^2]$	Height $[m]$	Hydraulic diameter $[m]$
Leibstadt				
Downcomer 1	6	10.330	5.073	1.160
Downcomer 2	6	0.720	4.384	0.128
Lower Plenum 1	2	9.260	6.000	6.100
Lower Plenum 2	3	10.510	1.790	0.300
Core Channel	25	Fuel type dependent		
Bypass		7.420		0.030
Riser	5	8.040	4.375	0.168
Steam Dome		20.960	8.460	5.170
Forsmark 1				
Downcomer 1	4	21.990	3.160	1.440
Downcomer 2	8	12.530	7.640	1.440
Lower Plenum 1	2	10.250	0.930	0.216
Lower Plenum 2	5	10.250	4.220	0.216
Core Channel	25	Fuel type dependent		
Bypass Channel		1.818		0.025
Riser	5	8.500	2.900	0.246
Steam Dome		25.540	8.540	10.000

Figure 3.4: Nodalization Scheme of the Leibstadt and Forsmark Reactors

3.1.2 Inconsistencies with the POLCA Model

In the beginning, MATSTAB was designed to use a steady state calculation of RAMONA as the starting point for its own calculations. The various data vectors (also called distributions) saved by RAMONA, such as cross sections, neutron fluxes, temperatures etc., could easily be loaded into MATSTAB, since the equations and parameters used were identical. This method was very convenient when comparing results. However, once trust in MATSTAB calculations was established, it was much simpler to use the distributions calculated from the online core simulator POLCA [1]. This simulator is used to overview various safety relevant numbers (e.g. thermal margins) and calculates the most recent state of the reactor core at least every half hour.

These distribution files are a natural starting point for all extended reactor calculations. As a matter of fact, also the input of RAMONA calculations is based on the very same files. Therefore, it is not only convenient but also logical to omit the RAMONA calculations in-between.

Unfortunately, the POLCA model differs somewhat from the neutronic model used in RAMONA, as it is optimized to reflect the current state of the reactor and not to investigate future transients. Since MATSTAB only needs a good steady state, use of either model is possible. In fact, the POLCA model is even more suitable, since its degree of sophistication is better adapted for steady state calculations.

The first attempt to use steady state data from POLCA distribution files as a base for MATSTAB calculations failed miserably. It took an in depth investigation to understand what went wrong, because the comparison between POLCA and RAMONA distributions showed good agreement.

The explanation, as far as we understand the problem today, lies in some non-obvious inconsistency of the data. Even though both sets of distributions fit their own equations well, there is a small discrepancy with respect to the equation of the other model. For example, the cross sections are only known to a certain precision. The same small error is reflected in a neutron flux calculation based on these cross sections. Now, if this neutron flux is inserted in the equations of the other model which differs in the calculation for boundary terms, one could readily argue that it also fits these equations assuming different cross sections. The new cross sections differ, however, more from the reality than their uncertainty allows. This leads to wrong results. The resulting error was that large, that the temperatures for the fuel zones were wrong by up to 100 degrees. Since all countermeasures to make the data consistent were in vain, the POLCA model was eventually coded into MATSTAB. Now the model used in MATSTAB is consistent with the steady state data used as input. The above explanation is also confirmed by the fact that the currently ongoing implementation of the POLCA 7 model [3] shows the same problems (POLCA 7 is a major update to POLCA 4 and uses a more detailed TH model as well as a two group neutronic model).

Since also the POLCA 4 model used in MATSTAB differs from the original POLCA 4 model by the simplifications introduced below, a few power-void iterations are executed to definitely adapt the input data to the model changes introduced in MATSTAB.

3.2 Neutron Kinetics and Power Generation

The original neutronic model from RAMONA or POLCA with eight differential equations per node (two energy groups and six delayed neutron groups) would represented a heavy computational burden. Especially the spatial coupling, which relates most of the roughly 9'000 nodes in a half-core case to its six neighbors, represented an obstacle which is expensive in computer time to overcome. Therefore, MATSTAB uses a slightly simplified neutronic model.

3.2.1 Fast and Thermal Neutron Flux

MATSTAB is based on a $1\frac{1}{2}$ energy group model (neglecting the divergence term of the thermal flux) with a simplified representation of the six delayed neutron groups. The power generation in the reactor core is calculated with full three-dimensional kinetics. Each individual fuel assembly is modeled separately and is subdivided into 25 axial nodes. For each fuel assembly, the burnup, the control rod history, the thermal parameters and the geometry e.g. spacers are given as an input. The operating point dependent data as nuclear cross-sections as well as many of the thermal hydraulic parameters are described as function of temperature, pressure and void etc.

The major changes with respect to POLCA are the use of the prompt jump approximation and a simplification of the precursor equation as shown below. For the complete derivation of all following equations see Appendix A. For convenience, the equations below are numbered the same way as in the Appendix.

The time derivative of the fast and the thermal flux are both set to zero, which means that the left hand side of A.14 and A.15 are set to zero.

$$\frac{1}{V_1}\frac{d\bar{\varphi}_{1n}}{d\tau} = -\sum_{m=1}^{6}\frac{1}{h_{nm}}\mathbf{J}_{1,nm} - (\Sigma_{a1}+\Sigma_r)\bar{\varphi}_{1n} + (1-\beta)\left(\nu_1\Sigma_{f1}\bar{\varphi}_{1n} + \nu_2\Sigma_{f2}\bar{\varphi}_{2n}\right) + \sum_d \lambda_d \bar{C}_d = 0 \tag{A.14}$$

$$\frac{1}{V_2}\frac{d\bar{\varphi}_{2n}}{d\tau} = -\sum_{m=1}^{6}\frac{1}{h_{nm}}\mathbf{J}_{2,nm} - \Sigma_{a2}\bar{\varphi}_{2n} + \Sigma_r\bar{\varphi}_{1n} = 0 \tag{A.15}$$

The prompt jump approximation is valid, if the life time of a neutron is much smaller than the studied phenomena. Physically it is an immediate adaption of the neutron flux to perturbations.

3.2.2 Delayed Neutrons

The life time of the precursors

$$\frac{d\bar{C}_{dn}}{d\tau} = \beta_d \left(\nu_1 \Sigma_{f1} \bar{\varphi}_{1n} + \nu_2 \Sigma_{f2} \bar{\varphi}_{2n}\right) - \lambda_d \bar{C}_{dn} \quad , \begin{matrix} d = 1,\ldots,6 \\ n = nodenumber \end{matrix} \tag{A.16}$$

is much closer to the time a density wave needs to pass the reactor than the neutron life time and, therefore, significant. The time derivative of the precursors may therefore not be set to zero. Nevertheless, it is possible to simplify equation A.16 without much loss in accuracy.

Equation 2.25 describes the time dependence of a state variable. For the variable $\bar{C_d}n(\tau)$ it reads as follows

$$\bar{C}_{dn}(\tau) = \bar{c}_{dn} e^{\lambda\tau} \tag{A.28}$$

where $\bar{c}_{dn}$ is a scalar and not time dependent. Equation A.16 may now be written as follows.

$$\frac{d\bar{c}_{dn} e^{\lambda\tau}}{d\tau} = \beta_d (\nu_1 \Sigma_{f1} \bar{\varphi}_{1n} + \nu_2 \Sigma_{f2} \bar{\varphi}_{2n}) - \lambda_d \bar{C}_{dn} \tag{A.29}$$

It is now possible to carry out the derivation with respect to time. This transforms the differential equation into an algebraic equation.

$$\lambda \bar{C}_{dn} = \beta_d (\nu_1 \Sigma_{f1} \bar{\varphi}_{1n} + \nu_2 \Sigma_{f2} \bar{\varphi}_{2n}) - \lambda_d \bar{C}_{dn} \tag{A.30}$$

Solving for $\bar{C}_{dn}$ yields

$$\bar{C}_{dn} = \frac{\beta_d}{\lambda - \lambda_d} (\nu_1 \Sigma_{f1} \bar{\varphi}_{1n} + \nu_2 \Sigma_{f2} \bar{\varphi}_{2n}) \tag{A.31}$$

$\bar{C}_{dn}$ is depending on λ which is unknown. Therefore, the starting guess of λ is used to calculate $\bar{C}_{dn}$. This simplification is good enough, as long as the starting guess for λ is reasonable. The draw back is however, that λ is complex and therefore the matrix $\mathbf{A}$ becomes complex too. It remains to mention that this simplification is used for the POLCA model as well as for the RAMONA model. Inserting A.31 into A.26 yields

$$\begin{aligned} 0 = &- \left[\sum_{m=1}^{6} \mathbf{X}_{1,nm} + \Sigma_{a1} + \Sigma_r \right] \bar{\varphi}_{1n} + \sum_{m=1}^{6} \mathbf{Y}_{1,nm} \bar{\varphi}_{1m} \\ &+ \tilde{\beta} (\nu_1 \Sigma_{f1} \bar{\varphi}_{1n} + \nu_2 \Sigma_{f2} \bar{\varphi}_{2n}) \end{aligned} \tag{A.32}$$

where

$$\tilde{\beta} = 1 - \beta + \sum_d \frac{\beta_d \lambda_d}{\lambda + \lambda_d} \tag{A.33}$$

Solving A.27 for $\bar{\varphi}_{2n}$ yields

$$\bar{\varphi}_{2n} = \frac{\left[\Sigma_r - \sum_{m=1}^{6} \mathbf{X}_{2,nm}\right]}{\Sigma_{a2}} \bar{\varphi}_{1n} + \frac{\sum_{m=1}^{6} \mathbf{Y}_{2,nm}}{\Sigma_{a2}} \bar{\varphi}_{1m}. \tag{A.34}$$

Inserting the solution into A.32 leads to

$$\begin{aligned} 0 = &- \left[\sum_{m=1}^{6} \mathbf{X}_{1,nm} + \Sigma_{a1} + \Sigma_r - \tilde{\beta}\nu_1\Sigma_{f1} - \tilde{\beta}\nu_2\Sigma_{f2}\frac{\left[\Sigma_r - \sum_{m=1}^{6}\mathbf{X}_{2,nm}\right]}{\Sigma_{a2}} \right] \bar{\varphi}_{1n} \\ &+ \left[\sum_{m=1}^{6} \mathbf{Y}_{1,nm} + \tilde{\beta}\nu_2\Sigma_{f2}\frac{\sum_{m=1}^{6}\mathbf{Y}_{2,nm}}{\Sigma_{a2}} \right] \bar{\varphi}_{1m} \end{aligned} \tag{A.35}$$

The algebraic equation A.35 which is the center of the neutronics in MATSTAB contains all information of the original eight differential equations besides the small differences introduced by the simplifications mentioned above.

3.3 Thermal Conduction

Associated with each neutronic node is an average fuel pin for which the thermal energy source and heat conduction are calculated. The calculated average fuel temperature feeds back into the neutronics (Doppler effect) and the calculated heat flux from the cladding surface enters the hydraulics calculations.

The thermal energy storage and conduction in the fuel pins, consisting of the fuel pellets, of the gas gap between pellet and cladding and of the fuel cladding is modeled with the following assumptions.

- Fuel and cladding are rigid, retaining their cylindrical geometries. Possible variations in time of the gas gap width can be taken into account by a temperature dependent gap conductance.
- The volumetric heat generation q'''_f is uniformly distributed over the fuel pellet cross section. Gamma heat generation in the gas gap and the cladding is ignored.
- Axial and azimuthal conduction is negligible
- The thermal properties like heat capacity, conductivity etc. can be represented with the correlations stated below.

3.4 Thermal-Hydraulics

The thermal-hydraulics model of RAMONA and hence of MATSTAB is a four-equation, non-homogeneous, non-equilibrium one-dimensional two-phase flow model with constitutive equations for thermodynamic state variables. Thermal non-equilibrium between the phases is accounted for by allowing the liquid in a two-phase mixture to depart from saturated conditions, while the vapor is assumed to be at saturation. Hydrodynamic non-equilibrium, i.e. un-equal velocities of the two phases, is introduced via a slip correlation.

3.5 Summary

MATSTAB uses a four-equation, non-homogeneous, non-equilibrium, one-dimensional, two-phase flow model for the thermal-hydraulics. The neutronic model is based on a $1\frac{1}{2}$ energy group approach with six delayed neutron groups. The power generation in the reactor core is calculated with full three-dimensional kinetics. Each individual fuel assembly is modeled separately and is subdivided into 25 axial nodes.

The fast and the thermal neutron flux are represented with algebraic equations. The precursors are also represented with algebraic equations, but using a more sophisticated approach. These simplifications are based on physical judgment and showed no significant influence on the calculation results.